Strong coupling corrections in the analysis of x-ray Thomson scattering measurements

2003 J. Phys. A: Math. Gen. 36 5971

(http://iopscience.iop.org/0305-4470/36/22/319)

INSTITUTE OF PHYSICS PUBLISHING JOURNAL OF PHYSICS A: MATHEMATICAL AND GENERAL

J. Phys. A: Math. Gen. **36** (2003) 5971–5980 PII: S0305-4470(03)55746-8

Strong coupling corrections in the analysis of x-ray Thomson scattering measurements

G Gregori, S H Glenzer and O L Landen

Lawrence Livermore National Laboratory, University of California, PO Box 808, CA 94551, USA

E-mail: gregori1@llnl.gov

Received 7 November 2002, in final form 15 January 2003
Published 22 May 2003
Online at stacks.iop.org/JPhysA/36/5971

Abstract

We present simplified expressions for the dynamic structure factor, or form factor $S(k, \omega)$, which is the quantity describing the inelastic x-ray scattering cross section from a dense plasma or a simple liquid. Our results, based on the random phase approximation (RPA) for the treatment on the charged particle coupling, are compared with analytical expressions for the free electron dynamic structure factor which include effects of strong coupling in both classical and degenerate plasmas. We will show that these modifications introduce minimal corrections to the RPA for typical conditions found in recent non-collective x-ray Thomson scattering experiment on solid density isochorically heated laser plasmas. On the other hand, strong collective scattering may exhibit significant deviations from the RPA. The results shown in this work can be applied to interpreting future x-ray scattering in warm dense plasmas occurring in inertial confinement fusion experiments or for the modelling of solid density matter found in the interior of planets.

PACS numbers: 52.70.La, 71.10.Ca, 61.10.Eq, 52.38.−r, 52.27.Gr, 61.20.Ne

1. Introduction

Microscopic diagnostics of dense plasmas pose several difficulties as currently adopted experimental techniques are rather limited in probing particle densities, temperatures and charge states of warm dense matter. Since dense plasmas are not transparent to UV or optical probes, they can only provide information on their surface layers. On the other hand, the emerging interest in understanding the properties of matter under extreme conditions, as the ones achieved in inertial confinement fusion (ICF) experiments [1], necessitates the development of finite temperature dense matter probes. In ICF implosion experiments, a variety of plasma regimes are created, and of particular interest are Fermi degenerate (or quantum) plasmas, characterized by a Fermi temperature greater than the electron kinetic

temperature. Moreover, equation of state (EOS) predictions for various degenerate plasmas can only be resolved by accurate measurements of the chemical state of the materials. However, uncertainties in the present data and the lack of reliable independent measurements of temperature and density have made the validation of current models and calculations difficult. The extension of spectrally resolved Thomson scattering [2] in the x-ray regime for the diagnostics of solid density plasmas has been recently presented both theoretically [3, 4] and experimentally [5]. This method was first discussed by Landen *et al* [3] as a viable diagnostic for ICF experiments. In [4], we have given a complete theoretical expression for the scattering form factor to represent x-ray Thomson scattering for arbitrary α parameter, where $\alpha = 1/k\lambda_D$ (λ_D is the Debye length) distinguishes between non-collective ($\alpha < 1$) and collective ($\alpha > 1$) scattering in classical plasmas. Extension to scattering from ideal, weakly coupled to degenerate plasmas was also extensively discussed by Gregori *et al* [4]. For plasmas obeying the classical statistics, the electron–electron coupling constant is defined as (see, e.g., Ichimaru [6]) $\Gamma \equiv \Gamma_{\text{clas}} = e^2/4\pi\epsilon_0 k_B T_e d$, where T_e is the electron temperature and $d = (3/4\pi n_e)^{1/3}$ the mean sphere radius per electron, with n_e the electron density. In other words, Γ_{clas} is the ratio between the potential and the kinetic energy of the electrons. In an ideal plasma, $\Gamma_{\text{clas}} \ll 1$ and the kinetic energy dominates the particle motion with negligible inter-particle coupling. In a strongly coupled plasma, $\Gamma_{\text{clas}} \gg 1$, and the electrostatic (Coulomb) forces determine the nature of the particle motion. Weakly-to-moderately coupled plasmas lie in the range $\Gamma_{\text{clas}} \lesssim 1$. The extension of definition of the coupling constant Γ to the quantum domain (i.e., a degenerate plasma) is discussed by Liboff [7]. In this case, quantum diffraction prevents the electrons from getting arbitrarily close to each other and Γ is now the ratio between the potential and the Fermi energy, $E_F = k_B T_F$, of the electrons. Having $E_F = \hbar^2(3\pi^2 n_e)^{2/3}/2m_e$, as electron density increases, in contrast to a classical plasma, the coupling constant decreases, since $\Gamma \equiv \Gamma_q = e^2/4\pi\epsilon_0 E_F d \sim n_e^{-1/3}$. Similarly, the definition of the scattering parameter α needs to be corrected to include quantum effects, such that $\alpha \sim 1/k\lambda_{TF}$ [4], where λ_{TF} is the Thomas–Fermi screening length.

Since in our previous work [4], the random phase approximation (RPA) was used in the derivation of the free electron dynamic structure, a validation of such an approach with more sophisticated techniques is necessary in the case of the analysis of x-ray scattering from weakly-to-moderately coupled plasmas ($\Gamma \lesssim 1$). In particular, we will obtain static and dynamic local field corrections to the RPA by using a simple pseudopotential description of the charged particle interaction in order to account for quantum diffraction and symmetry, and we will show that resultant corrections to the the dynamic structure are negligible for the experimental conditions found in recent x-ray Thomson scattering experiments [8, 5]. Conversely, we will also indicate possible future experiments which can exhibit significant differences from the RPA results.

2. Theory of x-ray Thomson scattering

We will briefly summarize the result of the theory [4] describing the x-ray scattering from a uniform plasma containing N ions per unit volume. If Z_A is the nuclear charge of the ion, the total number of electrons per unit volume in the system, including free and bound ones, is $Z_A N$. Let us now assume we probe such a system with x-rays of frequency ω_0 such that $\hbar\omega_0 \gg E_I$, with E_I the ionization energy of any bound electron, i.e., the incident frequency must be large compared to any natural absorption frequency of the scattering atom, which allows us to neglect photoabsorption. During the scattering process, the incident photon transfers momentum $\hbar\mathbf{k}$ and energy $\hbar\omega = \hbar^2 k^2/2m_e = \hbar\omega_0 - \hbar\omega_1$ to the electron, where ω_1

is the frequency of the scattered radiation. In the non-relativistic limit ($\hbar\omega \ll \hbar\omega_0$)

$$k = |\mathbf{k}| = \frac{4\pi}{\lambda_0}\sin(\theta/2) \tag{1}$$

with λ_0 the probe wavelength and θ the scattering angle. We denote with Z_f and Z_c the numbers of kinematically free and core electrons, respectively. Clearly, $Z_A = Z_f + Z_c$. To avoid possible confusions, we should stress that Z_f is conceptually different from the *true* ionization state of the atom. It includes both the truly free (removed from the atom by ionization) and the valence (weakly bound) electrons; thus $Z_f = Z + Z_v$, where Z is the number of electrons removed from the atom, and Z_v is the number of valence electrons. In the limiting case of a liquid metal, $Z = 0$, and only the valence (or conduction) electrons need to be considered. Following the approach of Chihara [9, 10], the scattering cross section is described in terms of the dynamic structure factor of all the electrons in the plasma

$$\frac{\mathrm{d}^2\sigma}{\mathrm{d}\Omega\,\mathrm{d}\omega} = \sigma_T\frac{k_1}{k_0}S(k,\omega) \tag{2}$$

where σ_T is the usual Thomson cross section and $S(k,\omega)$ is the total dynamic structure factor defined as

$$S(k,\omega) = |f_I(k) + q(k)|^2 S_{ii}(k,\omega) + Z_f S^0_{ee}(k,\omega) + Z_c\int \tilde{S}_{ce}(k,\omega-\omega')S_s(k,\omega')\,\mathrm{d}\omega'. \tag{3}$$

The first term in equation (3) accounts for the density correlations of electrons that dynamically follow the ion motion. This includes both the core electrons, represented by the ion form factor $f_I(k)$, and the screening cloud of free (and valence) electrons that surround the ion, represented by $q(k)$ [11]. $S_{ii}(k,\omega)$ is the ion–ion density correlation function. The second term in equation (3) gives the contribution in the scattering from the free electrons that do not follow the ion motion. Here, $S^0_{ee}(k,\omega)$ is the high-frequency part of the electron–electron correlation function [12] and it reduces to the usual electron feature [13, 14] in the case of an optical probe. Inelastic scattering by core electrons is included in the last term of equation (3), which arises from Raman transitions to the continuum of core electrons within an ion, $\tilde{S}_{ce}(k,\omega)$, modulated by the self-motion of the ions, represented by $S_s(k,\omega)$.

We shall also observe that for typical conditions in dense plasmas for ICF experiments, the ions are always non-degenerate, since their thermal de Broglie wavelength is much smaller than the average interparticle distance. On the other hand at $T_e \sim 0$, the electrons can exhibit some degree of degeneracy, and obey the Fermi–Dirac distribution. In order to describe the properties of a degenerate fluid, we use the approach suggested by Dharma-Wardana and Perrot [15] of treating the correlations by considering a *classical* Coulomb fluid at some effective temperature $T_q = T_F/(1.3251 - 0.1779\sqrt{r_s})$, with $r_s = d/a_B$ (a_B is the Bohr radius). The correlation properties are then calculated at the effective temperature $T_{cf} = \left(T_e^2 + T_q^2\right)^{1/2}$. This corrected temperature is chosen such that the temperature of an electron liquid obeying classical statistics exactly gives the same correlation energy of a degenerate quantum fluid at $T_e = 0$ obtained from quantum Monte Carlo calculations [16]. This approach was shown to reproduce finite-temperature static response of an electron fluid, valid for arbitrary degeneracy [16]. The reduction to a classical electron fluid problem also allows a unified definition of the coupling constant and the scattering parameter which is valid at any degeneracy [4]. In particular, we then have $\Gamma = e^2/4\pi\epsilon_0 k_B T_{cf} d$, and similarly $\alpha = 1/k\lambda_D = (\epsilon_0 k_B T_{cf}/e^2 n_e k^2)^{1/2}$, i.e., with the Debye length now calculated at the temperature T_{cf}. In the limit $T_e \to 0$, we thus have $\alpha \sim 1/k\lambda_{TF}$.

Under these conditions, and within the framework of the density response formalism for a two component plasma, we can calculate the static structure factors $S_{ii}(k)$, $S_{ee}(k)$ and

$S_{ei}(k) = S_{ie}(k)$ using the semi-classical approach suggested by Arkhipov and Davletov [17], which is based on a pseudo-potential model for the interaction between charged particles to account for quantum diffraction effects (i.e., the Pauli exclusion principle) and symmetry [18]. This approach was shown to give good agreement with the calculations of Ichimaru *et al* [19], based on the direct solution of the hypernetted chain (HNC) equations, up to $\Gamma \lesssim 1$ [17]. Under the assumption of thermodynamic equilibrium, the resultant expressions for the various static structure factors are thus:

$$S_{rs}(k) = \delta_{rs} - \frac{\sqrt{n_r n_s}}{k_B T_{cf}} \Phi_{rs}(k) \tag{4}$$

where $r, s = e$ (electrons) or i (ions), $n_e = Z_f n_i = Z_f N$. Symmetry in the electron–ion interactions requires $S_{ei}(k) = S_{ie}(k)$. The coefficients $\Phi_{rs}(k)$ are given by

$$\Phi_{ee}(k) = \frac{e^2}{\epsilon_0 \Delta}\left[\frac{k^2}{1+k^2\lambda_{ee}^2} + k_{Di}^2\left(\frac{1}{\left(1+k^2\lambda_{ee}^2\right)\left(1+k^2\lambda_{ii}^2\right)} - \frac{1}{\left(1+k^2\lambda_{ei}^2\right)^2}\right) + A\left(k^2 + \frac{k_{Di}^2}{1+k^2\lambda_{ii}^2}\right)k^2\exp(-k^2/4b)\right] \tag{5}$$

$$\Phi_{ii}(k) = \frac{Z_f^2 e^2}{\epsilon_0 \Delta}\left[\frac{k^2}{1+k^2\lambda_{ii}^2} + k_{De}^2\left(\frac{1}{\left(1+k^2\lambda_{ee}^2\right)\left(1+k^2\lambda_{ii}^2\right)} - \frac{1}{\left(1+k^2\lambda_{ei}^2\right)^2}\right) + \frac{Ak^2k_{De}^2}{1+k^2\lambda_{ii}^2}\exp(-k^2/4b)\right] \tag{6}$$

$$\Phi_{ei}(k) = -\frac{Z_f e^2}{\epsilon_0 \Delta}\frac{k^2}{1+k^2\lambda_{ei}^2} \tag{7}$$

where

$$b = \left(\lambda_{ee}^2 \pi \ln 2\right)^{-1} \qquad A = k_B T_{cf} \ln 2 \pi^{3/2} b^{-3/2} \epsilon_0 / e^2 \quad \text{and}$$

$$\Delta = k^4 + \frac{k^2 k_{De}^2}{1+k^2\lambda_{ee}^2} + \frac{k^2 k_{Di}^2}{1+k^2\lambda_{ii}^2} + k_{De}^2 k_{Di}^2\left(\frac{1}{\left(1+k^2\lambda_{ee}^2\right)\left(1+k^2\lambda_{ii}^2\right)} - \frac{1}{\left(1+k^2\lambda_{ei}^2\right)^2}\right) + Ak^2k_{De}^2\left(k^2 + \frac{k_{Di}^2}{1+k^2\lambda_{ii}^2}\right)\exp(-k^2/4b). \tag{8}$$

The inverse of the electron and the ion Debye lengths are $k_{De} = (n_e e^2/\epsilon_0 k_B T_{cf})^{1/2}$ and $k_{Di} = (Z_f n_e e^2/\epsilon_0 k_B T_{cf})^{1/2}$, respectively. In equations (5)–(8), the thermal de Broglie wavelength is defined by $\lambda_{rs} = \hbar/(2\pi\mu_{rs} k_B T_{cf})^{1/2}$ with $\mu_{rs} = m_r m_s/(m_r + m_s)$ the reduced mass of the interacting pair.

The first term in equation (3) describes the low-frequency response of the ions and since we cannot currently experimentally access this low-frequency part of the spectrum, we can simply approximate $S_{ii}(k, \omega) = S_{ii}(k)\delta(\omega)$. Thus, the calculation of the static structure factor for ion–ion correlations as described is quite reasonably correct for weakly-to-moderately couplings. Similarly, the response from tightly bound electrons within each single ion, the third term in equation (3), yields only a small background [4], at least for low-Z materials, and so its contribution on the resultant x-ray scattering spectrum can be neglected.

The free electron density–density correlation function that appears in the second term of equation (3) can be formally obtained through the fluctuation–dissipation theorem [20]:

$$S_{ee}^0(k, \omega) = -\frac{\hbar}{1 - \exp(-\hbar\omega/k_B T_e)}\frac{\epsilon_0 k^2}{\pi e^2 n_e}\mathrm{Im}\left[\frac{1}{\epsilon(k, \omega)}\right] \tag{9}$$

where $\epsilon(k,\omega)$ is the electron dielectric response function. In the case of an ideal classical plasma, the plasma dielectric response is evaluated from a perturbation expansion of the Vlasov equation [21]. The resultant form for the density correlation function is then known as the Salpeter electron feature [13]. This approach, however, fails when the electrons become degenerate or nearly degenerate as quantum effects begin to dominate. Under the assumption that inter-particle interactions are weak, so that the nonlinear interaction between different density fluctuations is negligible, the dielectric function can be derived in the RPA [22, 23]. In the classical limit, it reduces to the usual Vlasov equation. We shall stress the point that the RPA is derived under the assumption $\Gamma \ll 1$, thus its validity in the description of electron correlations in weakly-to-moderately coupled plasmas needs to be verified.

As a final remark on the validity of this approach, we have to stress that the plasma needs to be isotropic and homogeneous. Since, in inertial fusion experiments and other plasma experiments, this requirement is often not satisfied, a precise post-process analysis is necessary in order to deconvolve the data from the additional broadening induced by temperature and density gradients, which, in some instances, may account for all the relevant broadening observed in the experimental lineshapes. On the other hand, by carefully designing the experiment, it is possible to significantly reduce gradients in both density and temperature, thus reproducing uniform plasma conditions which are suitable for the analysis discussed in this paper, as, for example, in the recent experiments on spectrally resolved x-ray measurements on beryllium targets presented by Glenzer *et al* [5].

3. Local field corrections

The RPA form of the dielectric function is (see, e.g., Landau *et al* [21])

$$\epsilon_{RPA}(k,\omega) = 1 - v(k)\chi_0(k,\omega) \tag{10}$$

with $v(k) = e^2/\epsilon_0 k^2$ the Fourier transform of the bare Coulomb potential, and χ_0 is the density response of the non-interacting electron system:

$$\chi_0(k,\omega) = \frac{1}{\hbar}\int \frac{f(\mathbf{p}+\hbar\mathbf{k}/2) - f(\mathbf{p}-\hbar\mathbf{k}/2)}{\mathbf{k}\cdot\mathbf{p}/m_e - \omega - \mathrm{i}\nu}\frac{2\,\mathrm{d}^3p}{(2\pi\hbar)^3} \tag{11}$$

with $\nu \to 0^+$, thus neglecting any collisional effects. The electron distribution function is specified as

$$f(\mathbf{p}) = \frac{1}{\exp\left(\frac{p^2/2m_e-\mu}{k_B T_e}\right)+1} \tag{12}$$

where $\mathbf{p}$ is the electron momentum and μ the chemical potential, defined by the normalization condition

$$\int f(\mathbf{p})\frac{2\,\mathrm{d}^3p}{(2\pi\hbar)^3} = n_e \tag{13}$$

where we have accounted for both spin–state electrons.

Strong coupling effects stem from nonlinear correlations between density fluctuations and are usually described in terms of a dynamic local field correction (DLFC), $G(k,\omega)$, which measures the difference between the bare Coulomb interaction and the screened response [24]

$$\chi(k,\omega) = \frac{\chi_0(k,\omega)}{1 + v(k)G(k,\omega)\chi_0(k,\omega)} \tag{14}$$

and, $\epsilon(k,\omega) = 1 - v(k)\chi(k,\omega)$. Clearly, the RPA is reproduced for $G(k,\omega) = 0$. The calculation of the local field correction is not an easy task, and some approximations are

required. The most common one is to assume that $G(k,\omega)$ is a weak function of the frequency, thus $G(k) \equiv G(k,\omega=0)$ is the static local field correction (SLFC). In the one-component plasma approximation, the static local field correction is constrained at long and short wavelengths by the relations [6] $G(k\to 0)=\gamma(k/k_F)^2$ and $G(k\to\infty)=1-g(0)$, where $k_F=(3\pi^2 n_e)^{1/3}$ is the Fermi momentum, γ is a function of the compressibility and we typically have $\gamma\sim 1/4$ for $r_s\to 0$, i.e., for dense and ideal degenerate electron fluids. Similarly, $g(0)$ is the value of the radial distribution function at $r=0$ and $g(0)=1/2$ for $r_s\to 0$, while $g(0)\sim 0.1$ for the values of r_s appropriate for metallic densities [25]. By taking into account only the exchange contribution to the bare Coulomb potential, Hubbard [26] has proposed the following form of the SLFC for a degenerate ideal electron fluid ($r_s=0$) in the ground state ($T_e=0$):

$$G_H(k)=\frac{1}{2}\frac{k^2}{k^2+k_F^2}. \tag{15}$$

Since $G_H(k)$ does not satisfy the long wavelength boundary, and improved form was suggested by Geldart and Vosko [27]

$$G_{GV}(k)=\frac{1}{2}\frac{k^2}{k^2+2k_F^2}. \tag{16}$$

On the other hand, at values of $r_s>0$, neither (15) nor (16) may reproduce the correct long- and short-wavelength limits. In addition, at finite temperatures and especially when the electrons are in the state of intermediate degeneracy ($T_e\sim T_F$), exact representations of the local field correction are not available. Dandrea *et al* [25], extending the approach developed by Singwi *et al* [28] (STLS), have proposed a functional form of the type

$$G_D(k)=A\left(1-\mathrm{e}^{-Bk^2}\right) \tag{17}$$

where A and B are determined by the boundary conditions on $G(k)$. Similar results, also based on the work of Singwi *et al* [28], have been presented by Tanaka *et al* [29]. By contrast, as suggested by Dharma-Wardana and Perrot [15], the reduction of the quantum dynamics to a classical electron fluid via an effective temperature T_{cf} gives an explicit form for the SLFC by the classical relation

$$C_{ee}(k)=-\frac{v(k)n_e}{k_B T_{cf}}[1-G(k)] \tag{18}$$

where the electron–electron direct correlation function is obtained from the Ornstein–Zernike relations [30] in terms of the static structure factors

$$C_{ee}(k)=1-\frac{S_{ii}(k)}{S_{ee}(k)S_{ii}(k)-S_{ei}^2(k)}. \tag{19}$$

This allows the direct determination of $G(k)$ from the analytical static structures (4). In figure 1, we have compared the SLFC obtained from this approach with various different theoretical schemes for $n_e=10^{23}\,\mathrm{cm}^{-3}$ ($r_s=2.5$) and $T_e=T_F=7.86$ eV. At large wavelengths (small k), our approach seems to show a reasonable agreement with the Geldart and Vosko [27] result. We should mention that at $T=T_F$ and $r_s=2.5$ we have $\gamma\approx 0.3$ [16], thus the correct boundary condition is satisfied. Similarly, at large k, the short wavelength constraint is reproduced with sufficient accuracy.

Even if the static local field correction already gives a considerable improvement over the RPA, the full dynamic local field correction (DLFC) may be necessary for the correct modelling of strong coupling at frequencies $\omega\gtrsim\omega_{pe}$, where ω_{pe} is the electron plasma

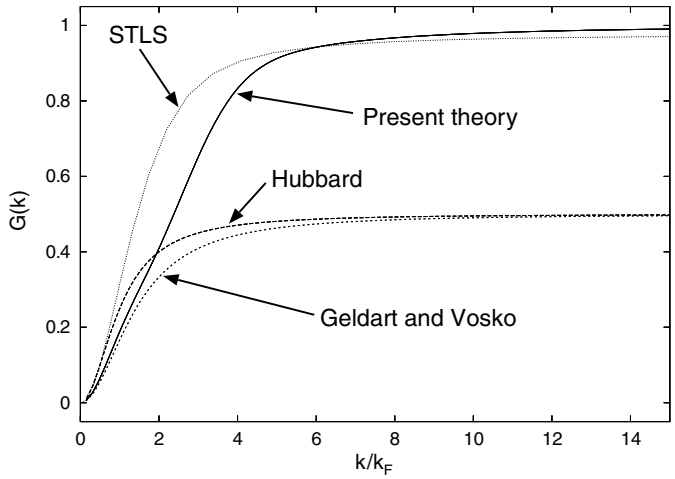

Figure 1. Static local field correction for $r_s = 2.5$ and $T_e/T_F = 1$ ($\Gamma = 0.99$) calculated for different theories: the present approach, given by equation (19); the Hubbard model; the Geldart and Vosko model and the STLS scheme in the Tanaka *et al* [29] extension.

frequency. Following the *ansatz* of Ichimaru *et al* [19], the DLFC is obtained from a simple interpolation of its low- and high-frequency limits

$$G(k,\omega) = \frac{\omega I(k) + \mathrm{i}\nu_e G(k)}{\omega + \mathrm{i}\nu_e} \tag{20}$$

where [19],

$$I(k) = -\frac{1}{n_e}\int \frac{\mathrm{d}^3 q}{(2\pi)^3}\frac{(\mathbf{k}\cdot\mathbf{q})^2}{k^2 q^2}[S_{ee}(|\mathbf{k}-\mathbf{q}|) - S_{ee}(q) + \sqrt{Z_f}S_{ei}(q)] \tag{21}$$

and

$$\nu_e = \frac{4\sqrt{2\pi}Z_f e^4 n_e}{3(4\pi\epsilon_0)^2\sqrt{m_e}(k_B T_{cf})^{3/2}}\ln\Lambda \tag{22}$$

is the effective electron–ion collision frequency [31]. The generalized Coulomb logarithm is given by [32]

$$\ln\Lambda = \int_0^\infty \frac{S_{ee}(k)S_{ii}(k) - S_{ei}^2(k)}{\left(1 + k^2\lambda_{ei}^2\right)^2}\frac{\mathrm{d}k}{k} \tag{23}$$

and, again, for the static properties we use the results from equation (4).

4. Results

In order to compare the RPA with the SLFC and DLFC given by equations (18) and (20), respectively, we use, as an example, a LiH ($Z_A = 4$, $Z_f = 2$) plasma with $n_e = 10^{23}$ cm^{-3} ($r_s = 2.5$, $T_F = 7.85$ eV) and two different electron temperatures: $T_e = 1$ eV and $T_e = 10$ eV. We have considered experimental conditions which are comparable to the ones achieved in typical laser plasma experiments [3, 8]. We assumed Ti He-α 4.75 keV radiation probe ($\lambda_0 = 0.26$ nm) at $\theta = 135^\circ$ scattering angle. Synthetic lineshapes for the free electron dynamic structure factor $S_{ee}^0(k,\omega)$ are plotted in figure 2. We see that the inclusion of either a SLFC or a DLFC has only a marginal effect on the form of the spectrum. This geometry

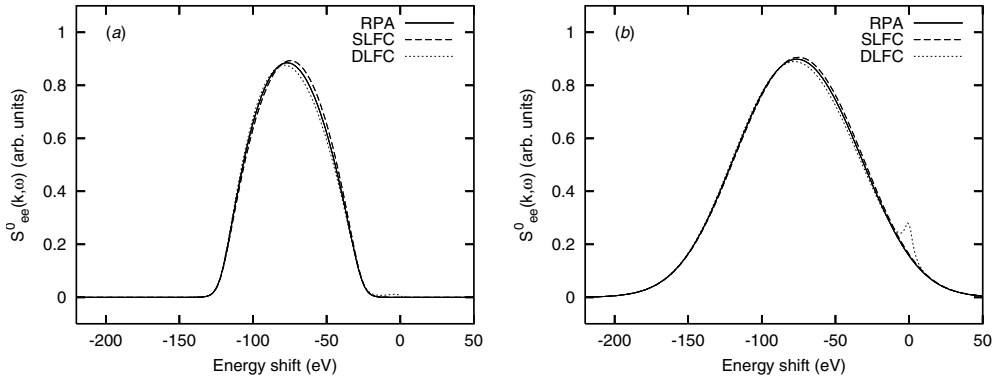

Figure 2. Free electron structure factor, $S^0_{ee}(k,\omega)$, for a LiH plasma with $Z_f = 2, r_s = 2.5$ and $T_e/T_F = 0.13$ (a) or $T_e/T_F = 1.3$ (b). The scattering wavenumber is $k/k_F = 3.1$, which corresponds to a scattering angle of $\theta = 135^\circ$ with an x-ray probe $\lambda_0 = 0.26$ nm. $\Gamma = 1.42$, $\alpha = 0.35$, $\nu_e/\omega_{pe} = 0.35$ (a) and $\Gamma = 0.86$, $\alpha = 0.27$, $\nu_e/\omega_{pe} = 0.31$ (b).

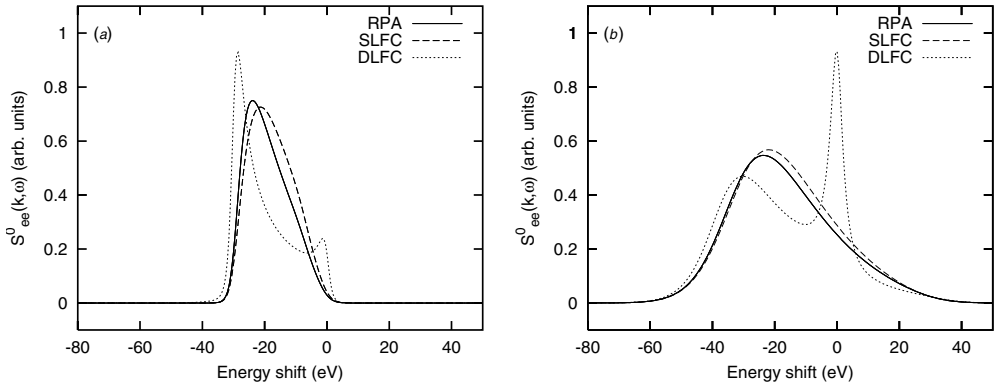

Figure 3. Free electron structure factor, $S^0_{ee}(k,\omega)$, for a LiH plasma with $Z_f = 2, r_s = 2.5$ and $T_e/T_F = 0.13$ (a) or $T_e/T_F = 1.3$ (b). The scattering wavenumber is $k/k_F = 0.87$, which corresponds to a scattering angle of $\theta = 30^\circ$ with an x-ray probe $\lambda_0 = 0.26$ nm. $\Gamma = 1.42$, $\alpha = 1.24$, $\nu_e/\omega_{pe} = 0.35$ (a) and $\Gamma = 0.86$, $\alpha = 0.96$, $\nu_e/\omega_{pe} = 0.31$ (b).

corresponds to the recent x-ray Thomson scattering experiments reported by Glenzer and co-workers [8, 5], thus confirming that in the analysis of those data, the RPA will provide fairly accurate results. We should note that at $\theta = 135^\circ$, the parameter α is less than unity (see figure 2) and the scattering probes the non-collective part of the spectrum, which is less sensitive to the microscopic correlations. On the other hand, at a scattering angle of $\theta = 30^\circ$, $\alpha \gtrsim 1$ (see figure 3), and such collective scattering is indeed more sensitive to the degree of interparticle coupling. This effect can be seen in figure 3 where the DLFC shows remarkable differences with the RPA. Conversely, the use of a static approximation is not able to capture the full effect of microscopic particle correlations. In this respect, we should observe that the SLFC relies on the low frequency approximation $G(k,\omega) \approx G(k,\omega = 0)$, which is typically valid when $\omega/\nu_e \ll 1$. However, at the considered electron density and temperature, the effective electron collision frequency is comparable to the electron plasma frequency (which is about 11 eV in energy units) and most of the spectrum develops in the region $|\omega| > \omega_{pe}$. At the same time, the collision-driven dynamics tend to enhance the low-frequency response with

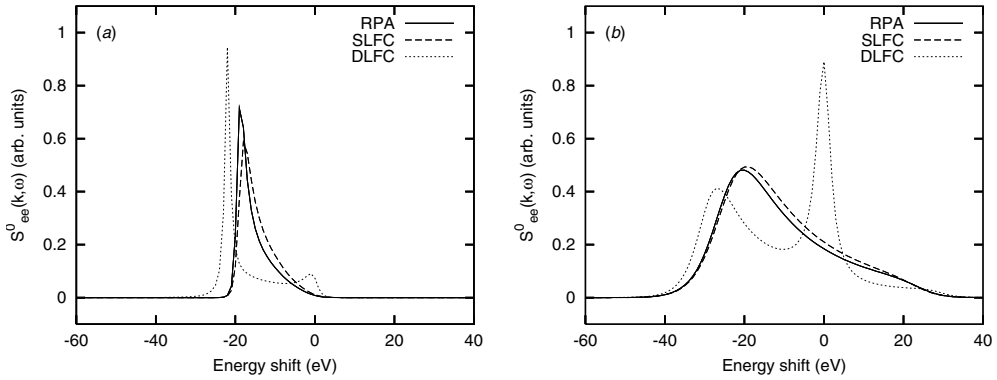

Figure 4. Free electron structure factor, $S^0_{ee}(k,\omega)$, for a LiH plasma with $Z_f = 2, r_s = 2.5$ and $T_e/T_F = 0.13$ (*a*) or $T_e/T_F = 1.3$ (*b*). The scattering wavenumber is $k/k_F = 1.2$, which corresponds to a scattering angle of $\theta = 135^\circ$ with an x-ray probe $\lambda_0 = 0.66$ nm. $\Gamma = 1.42$, $\alpha = 0.88$, $v_e/\omega_{pe} = 0.35$ (*a*) and $\Gamma = 0.86$, $\alpha = 0.69$, $v_e/\omega_{pe} = 0.31$ (*b*).

the appearance of an entropy peak [33] and thus the use of a DLFC becomes crucial. Figure 3 shows that indeed the DLFC results strongly diverge from the RPA or SLFC because of a more accurate accounting of collisional damping. Analogous conclusions are reached if instead we use a Si He-α 1.86 keV radiation probe ($\lambda_0 = 0.66$ nm) at $\theta = 135^\circ$ scattering angle for the same plasma conditions previously considered, as illustrated in figure 4. We clearly see that the use of a probe at longer wavelength, which enables sampling of the scattering towards the collective region of the spectrum (even in the advantageous backscattering geometry [3]) results again in large differences between the RPA and the local field corrected spectra.

5. Conclusion

We have discussed the effect of strong inter-particle coupling in the calculation of the free electron dynamic structure factor. The approach that we have followed enabled us to treat both classical and degenerate plasmas within the local field approximation. We have shown that both static and dynamic local field corrections introduce minimal modifications to the RPA structure factors for typical conditions found in recent x-ray Thomson scattering experiments on solid density laser plasmas [8, 5]. These experiments indeed correspond to non-collective scattering conditions where the overall spectral profile is weakly sensitive to the degree of coupling. On the other hand, at different experimental conditions corresponding to collective scattering geometries, significant departure from the RPA is observed. The results shown in this work can be applied to interpreting future x-ray scattering in warm dense plasmas occurring in inertial confinement fusion and high-energy density physics experiments and in the interior of planets.

Acknowledgments

This work was performed under the auspices of the US Department of Energy by the University of California Lawrence Livermore National Laboratory under contract no W-7405-ENG-48 and supported by Laboratory Directed Research and Development grant no 02-ERD-13.

References

[1] Lindl J D 1998 *Inertial Confinement Fusion* (New York: Springer)
[2] Glenzer S H *et al* 1999 *Phys. Rev. Lett.* **82** 97
[3] Landen O L *et al* 2001 *J. Quant. Spectrosc. Radiat. Transfer* **71** 465
[4] Gregori G, Glenzer S H, Rozmus W, Lee R W and Landen O L 2003 *Phys. Rev.* E at press
[5] Glenzer S H, Gregori G, Lee R W, Pollaine S M and Landen O L 2003 *Phys. Rev. Lett.* submitted
[6] Ichimaru S 1982 *Rev. Mod. Phys.* **54** 1017
[7] Liboff R L 1984 *J. Appl. Phys.* **56** 2530
[8] Glenzer S H 2001 *Bull. Am. Phys. Soc.* **46** 325
[9] Chihara J 1987 *J. Phys. F: Met. Phys.* **17** 295
[10] Chihara J 2000 *J. Phys.: Condens. Matter* **12** 231
[11] Riley D *et al* 2000 *Phys. Rev. Lett.* **84** 1704
[12] Ichimaru S 1973 *Basic Principles of Plasma Physics* (Reading, MA: Addison-Wesley)
[13] Salpeter E E 1960 *Phys. Rev.* **120** 1528
[14] Evans D E and Katzenstein J 1969 *Rep. Prog. Phys.* **32** 207
[15] Perrot F and Dharma-Wardana M W C 2000 *Phys. Rev.* B **62** 16536
[16] Dharma-Wardana M W C and Perrot F 2000 *Phys. Rev. Lett.* **84** 959
[17] Arkhipov Y V and Davletov A E 1998 *Phys. Lett.* A **247** 339
[18] Baus M and Hansen J-P 1980 *Phys. Rep.* **59** 1
[19] Ichimaru S, Mitake S, Tanaka S and Yan X-Z 1985 *Phys. Rev.* A **32** 1768
[20] Kubo R 1957 *J. Phys. Soc. Japan* **12** 570
[21] Landau L D, Lifshitz E M and Pitaevskii L P 1995 *Physical Kinetics* (Oxford: Pergamon)
[22] Pines D and Bohm D 1952 *Phys. Rev.* **85** 338
[23] Pines D and Nozieres P 1990 *The Theory of Quantum Fluids* (Redwood, CA: Addison-Wesley)
[24] Ichimaru S 1991 *Statistical Plasma Physics* (Reading, MA: Addison-Wesley)
[25] Dandrea R G, Ashcroft N W and Carlsson A E 1986 *Phys. Rev.* B **34** 2097
[26] Hubbard J 1957 *Proc. R. Soc. London* **243** A336
[27] Geldart D J W and Vosko S H 1966 *Can. J. Phys.* **44** 2137
[28] Singwi K S, Tosi M P, Land R H and Sjölander S 1968 *Phys. Rev.* **176** 589
[29] Tanaka S, Mitake S and Ichimaru S 1985 *Phys. Rev.* A **32** 1896
[30] Hansen J-P and McDonald I R 2000 *Theory of Simple Liquids* (London: Academic)
[31] Arkhipov Y V, Baimbetov F B, Davletov A E and Starikov K V 2000 *Phys. Scr.* **63** 194
[32] Baus M, Hansen J-P and Sjögren L 1981 *Phys. Lett.* **82** 180A
[33] Zhang Y Q, DeSilva A W and Mostovych A N 1989 *Phys. Rev. Lett.* **1848** 62